Reflection Colors

DOI: 10.1002/ange.201410788

Light-Directing Omnidirectional Circularly Polarized Reflection from Liquid-Crystal Droplets**

*Jing Fan, Yannian Li, Hari Krishna Bisoyi, Rafael S. Zola, Deng-ke Yang, Timothy J. Bunning, David A. Weitz, and Quan Li**

Abstract: *Constructing and tuning self-organized three-dimensional (3D) superstructures with tailored functionality is crucial in the nanofabrication of smart molecular devices. Herein we fabricate a self-organized, phototunable 3D photonic superstructure from monodisperse droplets of one-dimensional cholesteric liquid crystal (CLC) containing a photosensitive chiral molecular switch with high helical twisting power. The droplets are obtained by a glass capillary microfluidic technique by dispersing into PVA solution that facilitates planar anchoring of the liquid-crystal molecules at the droplet surface, as confirmed by the observation of normal incidence selective circular polarized reflection in all directions from the core of individual droplet. Photoirradiation of the droplets furnishes dynamic reflection colors without thermal relaxation, whose wavelength can be tuned reversibly by variation of the irradiation time. The results provided clear evidence on the phototunable reflection in all directions.*

Conferring remote and dynamic control to self-organized photonic structures with unique optical properties is currently a burgeoning area of research in the fabrication of smart stimuli-responsive soft materials and devices.[1] Toward this end, cholesteric liquid crystals (CLCs) have great promise in optics and photonics owing to their self-organized periodic helical superstructure.[2] Since the cholesteric liquid crystal is an anisotropic dielectric medium, its morphology causes a periodic modulation of the refractive index, thereby establishing a one-dimensional (1D) photonic band gap (PBG) centered at $\lambda = nP$, where P is the helical pitch and n is the average refractive index. In this wavelength region, light propagation is prohibited because the helical superstructure can selectively reflect circularly polarized light (CPL) of same handedness as that of the cholesteric liquid crystal. The pitch, the distance over which the director field rotates by 2π radians, is sensitive to external stimuli such as temperature, light, electric field, and mechanical stress.[2a] Of these stimuli, light is particularly fascinating owing to its advantages in offering remote, spatial, and temporal controllability in a wide range of ambient environments. Phototunability of the cholesteric liquid crystals' pitch and the circular polarized reflection wavelength has formed the basis of many applications including tunable color reflectors and filters, tunable lasers, optically addressed flexible displays without patterned electronics, and biomedical applications.[2] Usually cholesteric liquid crystals are investigated in planar geometries for both fundamental scientific studies as well as for device applications. Recently, the unusual and unique phenomena and properties arising from aplanar geometry, such as in droplets and microshells have been explored.[3] These studies suggest that the impact and scope of liquid-crystal applicability could be greatly enhanced by confining them into spherical geometries instead of the traditional thin films. Further fundamental studies are warranted as confinement can lead to appealing configurations within the droplet that reflect a fine balance between interfacial and elastic contributions to the free energy. In this endeavor has been made possible, thanks to the recent development of microfluidic techniques, the facile fabrication of stable three-dimensional (3D) droplets and microshells of anisotropic fluids in general and cholesteric liquid crystals in particular with controllable size and shell thickness.[4] Moreover, the microfluidic technique has enabled the size-polydispersity bottleneck in the fabrication of liquid crystal droplets to be overcome, thus opening the door for wider applications in advanced photonic devices.

Herein we report the fabrication and self-organization of photoresponsive cholesteric liquid crystal spherical droplets composed of a photosensitive chiral molecular switch (*S*,*S*)-**1** (Figure 1 A) with both a very high helical twisting power (HTP) and a large difference of the helical twisting powers between the initial (unirradiated) and UV irradiated photostationary states. Because of the high helical twisting power of

[*] Dr. J. Fan,[+] Prof. D. A. Weitz
School of Engineering and Applied Sciences
Harvard University, Cambridge, MA 02138 (USA)
Dr. Y. Li,[+] Dr. H. K. Bisoyi, Prof. D. Yang, Prof. Q. Li
Liquid Crystal Institute and Chemical Physics
Interdisciplinary Program, Kent State University
Kent, OH 44242 (USA)
E-mail: qli1@kent.edu
Prof. R. S. Zola
Departamento de Física
Universidade Tecnológica Federal do Paraná-Apucarana
PR 86812-460 (Brazil)
Dr. T. J. Bunning
Materials and Manufacturing Directorate
Air Force Research Laboratory
WPAFB, Dayton, OH 45433 (USA)
Prof. D. A. Weitz
Department of Physics, Harvard University
Cambridge, MA 02138 (USA)
[+] These authors contributed equally to this work.

[**] Q.L. thanks the AFOSR (FA9950-09-1-0193, FA9550-09-1-0254 and FA9550-12-1-0037) and the NSF (IIP 0750379). D.W. thanks the NSF (DMR-1310266), the Harvard Materials Research Science and Engineering Center (DMR-0820484), and Advanced Energy Consortium (BEG08-027).

Supporting information for this article is available on the WWW under http://dx.doi.org/10.1002/anie.201410788.

 © 2015 Wiley-VCH Verlag GmbH & Co. KGaA, Weinheim

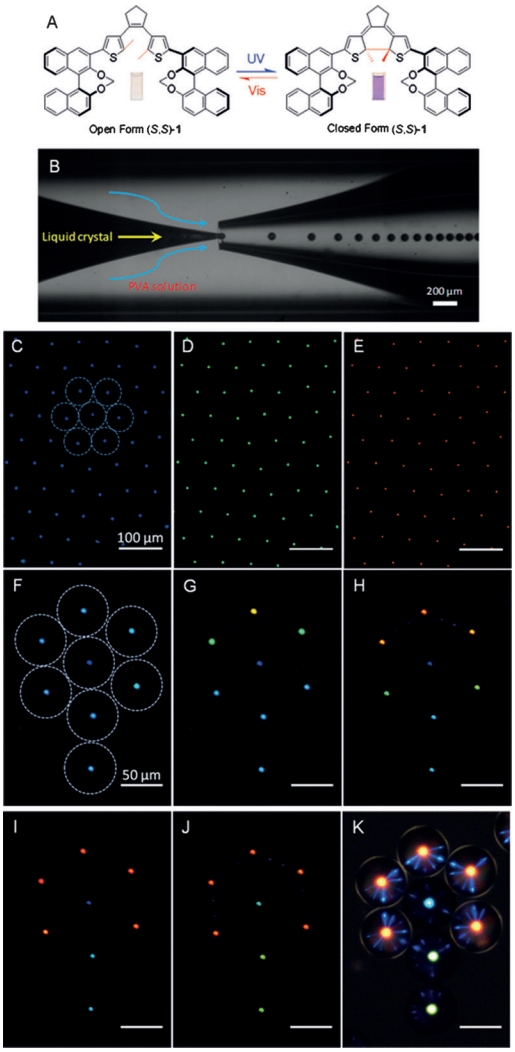

Figure 1. Fabrication and omnidirectional reflections of monodisperse liquid-crystal droplets. A) Photoisomerization of the chiral switch (*S*,*S*)-**1** which was doped in E7 to form the cholesteric liquid crystal. Inset: the color change of (*S*,*S*)-**1** from colorless to purple upon UV irradiation. B) Fabrication of the monodisperse chiral liquid-crystalline droplets from the 1D cholesteric liquid crystal by using a glass capillary-based microfluidic device. Droplets are supported and surrounded by 10% PVA aqueous solution. C)–K) Reflection-mode cross-polarized microscope images. C)–E) Hexagonal arrays of droplets show full range red, green, and blue colors upon shining $\lambda = 546$ nm light on the UV-irradiated photostationary state (blue). Dash circles in panel (C) indicate the positions of seven drops in hexagonal close packing. F)–K) a group of eight monodisperse photoresponsive droplets with light-driven iridescent colors. The dash circles in panel (F) indicate the positions of the eight droplets. Panels (F—K) show the results of shining $\lambda = 546$ nm visible light on selected droplets in the UV-irradiated photostationary state for different times. Panel (K) is at the same state with panel (J) but taken at a higher gain value.

the chiral dopant, a small amount is enough to fabricate photoresponsive cholesteric liquid crystals without significantly altering the optimized properties of the commercially available achiral liquid crystal host E7. The large difference in helical twisting power between both isomeric states enables a wide range tunability of the pitch (and thus selective reflection wavelength) of the cholesteric liquid crystal fluid. The resulting 3D droplets with radial orientation of the helical axes are monodisperse in size and produce omnidirectional Bragg reflections encompassing red, green, and blue (RGB) colors. The selective circularly polarized reflection colors can be reversibly tuned by light irradiation, and red, green, and blue colors can be realized from the same droplet by controlling the photoirradiation time. Furthermore, they organize into hexagonal assemblies with interesting lateral cooperative photonic interactions.

Chiral diarylethene switch (*S*,*S*)-**1** was prepared by a facile synthesis procedure (see Supporting Information Figure S1).[5] Its photocyclization process exhibits photochemically reversible but thermally stable behavior in organic solvents (Figure S2). Upon UV irradiation, the helical twisting power (molar %) value of (*S*,*S*)-**1** in E7 increases from 104 μm^{-1} to 153 μm^{-1} (i.e. a blue shift in color) which can be almost returned back to its initial state of 105 μm^{-1} helical twisting power upon visible light irradiation at 550 nm. To fabricate monodisperse spherical cholesteric liquid crystal drops, we used a glass capillary-based microfluidic device consisting of two tapered cylindrical capillaries coaxially assembled into a square capillary (Figure 1 A). The dispersed phase is the photoresponsive cholesteric liquid crystal composed of 2.4 mol % of (*S*,*S*)-**1** in liquid crystal E7. To implement stable generation of monodisperse droplets, the cholesteric liquid crystal is heated above its clearing point to reduce its viscosity. The continuous phase is a 10 wt % poly(vinyl alcohol) (PVA) aqueous solution which not only stabilizes the cholesteric liquid crystal droplets against coalescing but also facilitates the planar anchoring of the liquid crystal molecules at the droplet surfaces resulting in the radial orientation of the helical axes within the droplets (Figure S4). By adjusting the flow rates of both phases, we fabricate monodisperse cholesteric liquid crystal droplets of approximately 50 μm diameter and collect them in a chamber (125 μm thick controlled by spacers) consisting of two parallel glass slides. The chamber is sealed using epoxy to avoid evaporation of the supporting continuous aqueous phase. As a result of the identical size (monodispersity) of the spherical droplets, a hexagonal close packed structure is formed spontaneously, either as a coplanar single-layer or a stacked double-layer depending on the droplet volume fraction and the container chamber thickness.

The central (core) region of the droplet exhibits the color of normal incidence selective circularly polarized reflection from the cholesteric liquid crystal,[3m] which confirms the radial orientation of the helical axes inside the spherical droplets. The helical twisting power of (*S*,*S*)-**1** increases upon UV irradiation and hence blue-shifts the initial red color. Thus, for a single layer of hexagonally close-packed cholesteric liquid-crystal droplets, after shining UV light of $\lambda = 310$ nm for approximately 1 min, the droplets change their reflection from the initial red to a photostationary blue. The initial red color can be restored from the UV-irradiated state by shining $\lambda = 546$ nm visible light at the intensity of 30 mW cm^{-2} for 1.5 min. Figure 1 C–E show the reflection images of a monolayer hexagonal packing of cholesteric

 © 2015 Wiley-VCH Verlag GmbH & Co. KGaA, Weinheim

liquid-crystal droplets with blue (C), green (D), and red (E) colors in the central spots, respectively. The bright spot is the region from where CPL is reflected. The size of the central bright spot is about 5 μm, much smaller than the droplet size (ca. 50 μm).

Owing to the stability of individual droplets in the colloidal array, we are able to spatially and remotely control the color of selected droplets independently. This enables fine-tuning the color pattern of groups of droplets by the programmed shining of light of the desired wavelength for different times to pre-selected droplets, as shown in Figure 1 F–K. Figure 1 F shows an array of eight droplets (indicated by 8 dashed circles) in the shape of a flower with petals above a general stem. The central spot of each drop, blue, was formed at the $\lambda = 310$ nm UV irradiated photostationary state. By shining $\lambda = 546$ nm light at 30 mW cm^{-2} on selected drops for different times, the color of each "petal" can be changed to green, yellow, orange, and red, respectively, as shown in Figure 1 F–I. Light is then shined on all eight drops for an additional 20 s leaving the five red petals' color unchanged because they have already fully recovered to the initial state, yet changing the colors of the droplets representing the flower core and stem (Figure 1 J). Figure S5 presents another two examples of colorful patterns obtained by selective irradiation to different areas of hexagonal monolayer drop packing.

Interestingly, if we use a higher gain value when recording the polarized microscope images (Figure 1 J), we observe both the bright central spots in each drop and some additional radial blue lines in the red petals, as shown in Figure 1 K. We attribute the origin of this peripheral light pattern of blue lines to lateral photonic cross-talk between the droplets. The mechanism behind the cross-talk is shown in Figure 2 A,B. According to Bragg's law of reflection, the center wavelength obeys the rule $\lambda = nP\cos\theta$, where θ is the angle between the helix axis and the light propagation direction. When $\theta \approx 0°$, red light with wavelength nP is reflected from the droplet's core as shown in Figure 2 A (red arrow). Light that hits the periphery (or inside the droplet shown by the dotted ray) makes a non-zero incident angle with the helical axes because of the curvature, which causes an angle-dependent blue-shift from $\lambda = nP$. A cholesteric liquid crystal of defined pitch can selectively reflect light of different wavelengths depending on the angle of incidence of the light with respect to the helix axis.[6] When $\theta \approx 45°$, light is reflected from the left droplet to the right droplet as depicted by the blue arrow in Figure 2 A. The reflected light from the first droplet is circularly polarized with the same sense as the neighbor so all the light incident from the first one is directed to the objective by the neighboring droplet. If, for example, $nP = 650$ nm, the reflected ray of this cross-talk is $\lambda \approx 460$ nm for $\theta \approx 45°$. Drops with shorter pitch therefore have blue-shifted cross-talk rays, getting bluer until it eventually goes out of the visible spectrum, which is observed for the cyan and green droplets. This also explains the lack of, or little, cross-talk between droplets of different pitches (Figure 1 K).

To corroborate the above hypothesis, we isolated one, two, three, four, and five droplets, respectively, as five individual groups as shown in Figure 2 C–G. The isolated single droplet only exhibits the central reflection spot because of the absence of any lateral communication. The reflection-based interaction between neighboring droplets can be identified in the groups of two or more droplets. We also found that the intensity of photonic cross-interaction becomes weaker or stronger depending on the distance between two nearby droplets, and nearly disappears or is not noticeable when the distance is larger than approximately five-times the droplet diameter (see Figure 3). When the monodisperse droplets densely pack into a mono-layer with hexagonal symmetry, cross-communication with the six nearest neighbors and six penultimate neighbors forms a circular "lit fire-cracker" pattern as shown in Figure 2 H. These observations of lateral

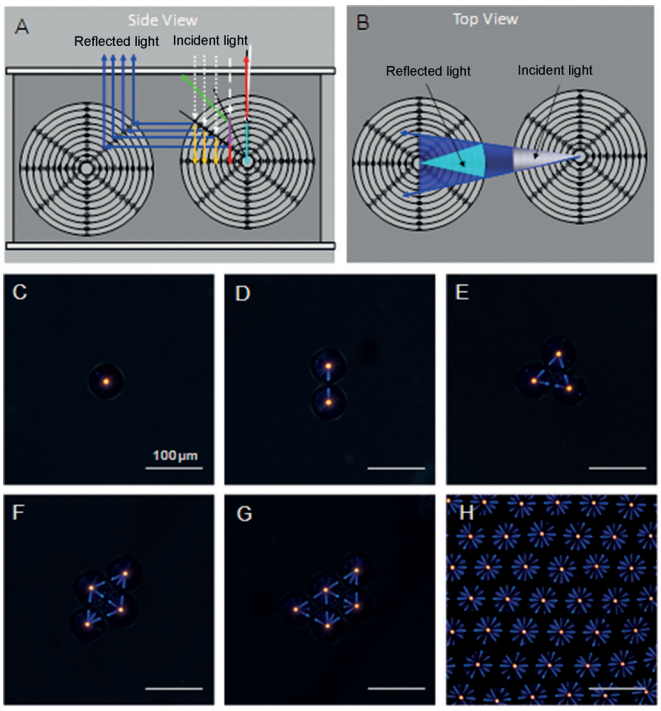

Figure 2. Schematic mechanism and evidence of omnidirectional reflection of the monodisperse droplets. A) Light incident at the center of the droplet is reflected back with the same wavelength as the selective reflection of the cholesteric liquid crystal. As a result of the curvature, light that makes an angle of approximately 45° with the helical axis (which happens at the periphery or inside the droplet) is reflected toward the neighboring droplet. It is then reflected and directed to the observer, represented by the dotted arrows (white incident light) and the blue arrows (reflected cross-communication). Incident light that makes an angle between 0° and 45° is reflected in a wavelength between the observed central spot and cross-communication colors, but it is not collected by the microscope's acceptance cone, as shown by the green arrow. The arrows pointing down represent the wavelengths not reflected by the photonic band-gap and therefore pass through the droplet. B) The helical organization, observed from the top, responsible for the cross-communication, and the reflection pattern dictated by the cholesteric's reflection and the droplet curvature. C)–H) Reflection-mode cross-polarizing microscopic images of the droplets in the photostationary state. The appearance of linear-, triangular-, and diamond-shaped blue ray patterns in groups of droplets with one, two, or three nearest-neighbor droplets, respectively, indicates that they originate from photonic cross-communication between the surrounding droplets.

© 2015 Wiley-VCH Verlag GmbH & Co. KGaA, Weinheim

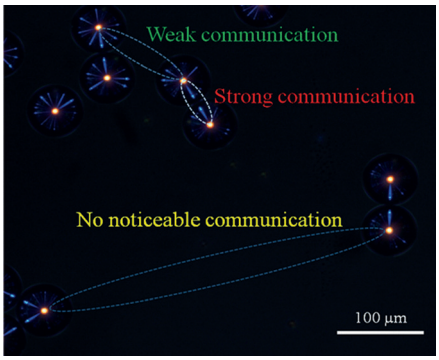

Figure 3. Distance-dependent strength of photonic communication between cholesteric liquid-crystal droplets.

photonic communication support the omnidirectional reflection of light from the core of the droplets and explains the origin of intra-drop radial blue line light patterns.

We extend our investigation to a double-layer hexagonal packing of monodisperse cholesteric liquid-crystal droplets. Since the stack can be irradiated from either side with a different (preselected) wavelength, the color pattern of each layer can be independently addressed. As an example, we (in Figure 4C,G) start with a top layer of blue droplets and a bottom layer of cyan droplets. In Figure 4C, the light is focused on the top layer while Figure 4G shows the image when the light is focused on the bottom layer. Dashes are drawn around the top layer droplets in Figure 4C. Upon shining visible light from the top, the top layer of droplet cores change color from blue to green while the bottom layer changes color from cyan to green as a result of a smaller exposure area or weaker light intensity. Two layers of green droplets are shown in Figure 4D,H at different focus planes. Additional irradiation yields an image where the top layer exhibits red cores and the bottom layer exhibits orange cores (Figure 4F,J).

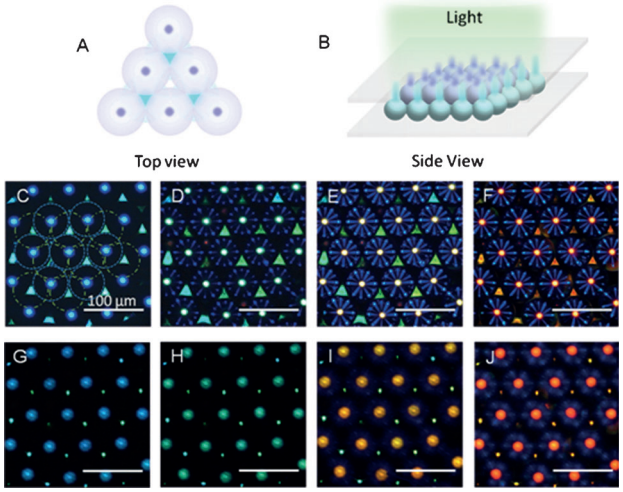

Figure 4. A) and B) Schematic representation of the droplet arrangement. C)–J) Reflection-mode cross-polarized microscope images of double-layer hexagonal droplet packing. The dash circles in panel (C) indicate the positions of the droplets. In panels (C–F), the light focuses on the top layer of droplets, which show bright central spots with blue communication arrays in panels (D–F). The bottom layer of droplets appears bright triangles in the interstices of the top layer. Panels (G–J) are at the same state as panels (C–F) respectively, with the light focusing on the bottom layer of droplets. See text for details.

In summary, we fabricated monodisperse photoresponsive cholesteric liquid-crystal droplets containing a photosensitive chiral molecular switch with large helical twisting power. The assembly was performed using a capillary-based microfluidic technique. Owing to the large change in the helical twisting power upon irradiation, the molecular switch enables a wide tuning of the pitch and hence of the circularly polarized reflection wavelength emanating from the droplets which have a radial orientation of the helical axes. Omnidirectional RGB reflection colors have been attained from the droplets by variation of the exposure time. The reflection colors are thermally stable because of the thermal bistability of the open and closed isomeric forms of the chiral molecular switch. Multicolor complex patterns can be achieved and lateral interaction between neighboring droplets yield complex, yet controllable, beautiful images in two-dimensional hexagonal groupings of droplets. The cross communication is a unique property of the system presented herein, owing to the combination of Bragg reflection, the droplet's curvature, and size. The monodisperse liquid-crystalline droplets and their arrays may find application in photonic devices where generation and exploitation of circularly polarized light with tunable wavelength is desired. Furthermore, these photoresponsive microdroplets are rich platforms for fundamental theoretical studies in understanding geometric confinement of stimuli-responsive soft materials.

Received: November 5, 2014
Published online: December 8, 2014

Keywords: color · microfluidics · omnidirectional selective reflection · liquid-crystal droplets · photonic crystals

[1] a) *Intelligent Stimuli Responsive Materials: From Well-Defined Nanostructures to Applications* (Ed.: Q. Li), Wiley, Hoboken, **2013**; b) *Nanoscience with Liquid Crystals: From Self-Organized Nanostructures to Applications* (Ed.: Q. Li), Springer, Heidelberg, **2014**.

[2] a) H. K. Bisoyi, Q. Li, *Acc. Chem. Res.* **2014**, *47*, 3184; b) Y. Wang, Q. Li, *Adv. Mater.* **2012**, *24*, 1926; c) D. J. Mulder, A. P. H. J. Schenning, C. W. M. Bastiaansen, *J. Mater. Chem. C* **2014**, *2*, 6695; d) N. Tamaoki, *Adv. Mater.* **2001**, *13*, 1135; e) S. Pieraccini, S. Masiero, A. Ferrarini, G. P. Spada, *Chem. Soc. Rev.* **2011**, *40*, 258.

[3] a) I. H. Lin, D. S. Miller, P. J. Bertics, C. J. Murphy, J. J. de Pablo, N. L. Abbott, *Science* **2011**, *332*, 1297; b) J. Chen, E. Lacaze, E. Brasselet, S. R. Harutyunyan, N. Katsonis, B. L. Feringa, *J. Mater. Chem. C* **2014**, *2*, 8137; c) H. F. Gleeson, T. A. Wood, M. Dickinson, *Philos. Trans. R. Soc. London Ser. A* **2006**, *364*, 2789; d) Y. Uchida, Y. Takanishi, J. Yamamoto, *Adv. Mater.* **2013**, *25*, 3234; e) M. Humar, I. Musevic, *Opt. Express* **2010**, *18*, 26995; f) P. P. Crooker, D. K. Yang, *Appl. Phys. Lett.* **1990**, *57*, 2529; g) J. D. Lin, M. H. Hsieh, G. J. Wei, T. S. Mo, S. Y. Huang, C. R. Lee, *Opt. Express* **2013**, *21*, 15765; h) G. Cipparrone, A. Mazzulla, A. Pane, R. J. Hernandez, R. Bartolino, *Adv. Mater.* **2011**, *23*, 5773; i) D. J. Gardiner, S. M. Morris, P. J. W. Hands, C. Mowatt, R.

 © 2015 Wiley-VCH Verlag GmbH & Co. KGaA, Weinheim

Rutledge, T. D. Wilkinson, H. J. Coles, *Opt. Express* **2011**, *19*, 2432; j) P. J. W. Hands, D. J. Gardiner, S. M. Morris, C. Mowatt, T. D. Wilkinson, H. J. Coles, *Appl. Phys. Lett.* **2011**, *98*, 141102; k) D. Wenzlik, C. Ohm, C. Serra, R. Zentel, *Soft Matter* **2011**, *7*, 2340; l) D. Seč, T. Porenta, M. Ravnik, S. Žumer, *Soft Matter* **2012**, *8*, 11982; m) J. Noh, H. L. Liang, I. Drevensek-Olenik, J. P. F. Lagerwall, *J. Mater. Chem. C* **2014**, *2*, 806; n) F. Xu, P. P. Crooker, *Phys. Rev. E* **1997**, *56*, 6853; o) L. Chen, Y. Li, J. Fan, H. K. Bisoyi, D. A. Weitz, Q. Li, *Adv. Optical Mater.* **2014**, *2*, 845.

[4] a) T. Lopez-Leon, A. Fernandez-Nieves, *Colloid Polym. Sci.* **2011**, *289*, 345; b) A. S. Utada, L. Y. Chu, A. Fernandez-Nieves, D. R. Link, C. Holtze, D. A. Weitz, *MRS Bull.* **2007**, *32*, 702.

[5] Y. Li, A. Urbas, Q. Li, *J. Am. Chem. Soc.* **2012**, *134*, 9573.

[6] H. Nemati, D. K. Yang, K. L. Cheng, C. C. Liang, J. W. Shiu, C. C. Tsai, R. S. Zola, *J. Appl. Phys.* **2012**, *112*, 124513.

 © 2015 Wiley-VCH Verlag GmbH & Co. KGaA, Weinheim